JOURNAL OF SPACECRAFT AND ROCKETS
Vol. 37, No. 3, May–June 2000

Nonequilibrium Vibrational Kinetics of an O_2/O Mixture Hitting a Catalytic Surface

Iole Armenise,* Mario Capitelli,† Claudine Gorse,‡ Mario Cacciatore,§ and Maria Rutigliano¶
University of Bari, 70126 Bari, Italy

The importance of a silica surface in affecting both the state-to-state kinetics and the macroscopic properties of an O_2/O mixture hitting a blunt body at hypersonic speed has been investigated. First, the surface has been considered catalytic only for recombination: three different assumptions are examined and compared with the results from a noncatalytic surface model. Second, both deactivation and dissociation are treated in the framework of a catalytic surface.

Nomenclature

C_a = ρ_a/ρ
C_M = ρ_M/ρ
C_v = ρ_v/ρ
C_{wa} = ρ_{wa}/ρ_w
$D_{(M/a)m}$ = diffusion coefficient of the species M/a in the mixture, $m^2\ s^{-1}$
E_{kin} = impinging atom kinetic energy, eV
f = stream function
K_{wa} = catalyticity, $m\ s^{-1}$
k = Boltzmann constant, JK^{-1}
P = pressure, $N\ m^{-2}$
P_{E-R} = Eley–Rideal probability
Pr = Prandtl number
Sc = Schmidt number
S_T = source term of the energy equation
S_v = source terms of the continuity equations
T = temperature, K
u_e = flow velocity along the surface, $m\ s^{-1}$
$w_{M/a}$ = molecular/atomic variation rate due to the recombination on the surface, $kg\ m^{-2}\ s^{-1}$
β = du_e/dx, s^{-1}
γ = recombination coefficient
γ_{deact} = deactivation probability
γ_{diss} = dissociation probability
γ_v = recombination coefficient in the vibrational level v
η = coordinate normal to the surface
θ = T/T_e
λ' = thermal conductivity coefficient, $W\ m^{-1}\ K^{-1}$
ρ = total density, $kg\ m^{-3}$
ρ_v = density in the vth vibrational level, $kg\ m^{-3}$
ρ_w = total density at the wall, $kg\ m^{-3}$

Subscripts

a = atom
e = external edge of the boundary layer
M = molecule
v = vth vibrational level
w = wall

Presented as Paper 99-3631 at the AIAA 33rd Thermophysics Conference, Norfolk, VA, 28 June–1 July 1999; received 10 August 1999; revision received 21 February 2000; accepted for publication 22 February 2000.

*Researcher, Centro Studio Chimica dei Plasmi del Consiglio Nazionale delle Ricerche, via Orabona 4. Member AIAA.
†Professor, Dipartimento di Chimica, via Orabona 4. Member AIAA.
‡Professor, Dipartimento di Chimica, via Orabona 4.
§Research Director, Centro Studio Chimica dei Plasmi del Consiglio Nazionale delle Ricerche, via Orabona 4.
¶Researcher, Centro Studio Chimica dei Plasmi del Consiglio Nazionale delle Ricerche, via Orabona 4.

Introduction

NONEQUILIBRIUM vibrational kinetics coupled to dissociation recombination processes have been recently investigated for conditions typically met in the boundary layer of a body traveling at hypersonic speed.[1–6] These studies so far have been restricted to noncatalytic surfaces, either for atom recombination or for vibrational energy accomodation.

The assumption of a noncatalytic surface is, of course an approximation, justified only by the lack of information about state-to-state recombination and deactivation rates of atomic and molecular species on the surface. Through a molecular dynamic approach, recently Cacciatore et al.[7,8] studied the recombination of atomic oxygen on silica, that is, the reaction of

$$O + O^*SiO_2 \rightarrow O_2(v) + SiO_2$$

which also gives the nascent distribution function of molecular oxygen after catalytic recombination. The relevant state-to-state rates can be inserted in the boundary-layer code developed in Refs. 1–6 to describe the role of vibrationally specific surface recombination on the whole nonequilibrium vibrational kinetics.

Such an approach is completely innovative because the catalicity in computational fluid dynamics codes is usually treated on a phenomenological basis completely disregarding the possibility of forming vibrationally excited states.

The paper describes the role of the recombination process and of the deactivation of vibrationally excited molecules on the surface in affecting vibrational distributions, molecular and atomic population densities, and temperature gradient. The last quantity can have practical implications in determining heat flow on the surface and, therefore, on the thermal protection system of reentry bodies.

Catalytic Effects

It is now well accepted that atom recombination on a surface can occur through two mechanisms[7–10]: the Eley–Rideal mechanism and the Langmuir–Hinshelwood mechanism. In the Eley–Rideal mechanism, an atom in the gas phase, A, hitting an adatom of the surface, A^*, produces a molecule in the gas phase, A_2, which generally will be vibrationally excited [$A_2(v)$]:

$$A + A^* \rightarrow A_2(v) + \text{wall} \tag{1}$$

In the Langmuir–Hinshelwood mechanism, two adatoms A^* moving on the surface recombine producing molecules in the gas phase:

$$A^* + A^* \rightarrow A_2(v) + \text{wall} \tag{2}$$

The process rate due to recombination on the surface can be written as

$$w_a = K_{wa}\rho_w C_{wa} \tag{3}$$

where

$$K_{wa} = \gamma\sqrt{kT_w/2\pi m} \tag{4}$$

is the catalyticity, that is, the surface catalytic recombination rate and γ is the recombination coefficient,[7,8] that is, the ratio of the flux of atoms recombining on the surface over the flux of atoms impinging the surface.

To consider a partially catalytic surface, the boundary condition should be written

$$w_{M/a} = \rho_w D_{(M/a)m} \left.\frac{\partial C_{M/a}}{\partial \eta}\right|_w \tag{5}$$

where $D_{(M/a)m}$ is the diffusion coefficient of the species M/a, that is, either of the molecules or of the atoms, in the mixture.

The equations satisfied on the surface as boundary conditions follow from Eqs. (3–5):

$$\left.\frac{\partial C_a}{\partial \eta}\right|_w = \frac{\gamma}{D}\sqrt{\frac{kT}{2\pi m}} \cdot C_a, \qquad \left.\frac{\partial C_M}{\partial \eta}\right|_w = -\frac{\gamma}{D}\sqrt{\frac{kT}{2\pi m}} \cdot C_a \tag{6}$$

In the following, γ will be called the global recombination coefficient, that is, it describes the recombination coefficient for the recombination reactions

$$O + O^* \rightarrow O_2(v) + \text{wall}, \qquad O^* + O^* \rightarrow O_2(v) + \text{wall} \tag{7}$$

without taking into account the vibrational level of O_2 involved in the recombination process. The recombination is achieved in the framework of the global coefficient approach by considering two limiting conditions: The first one assigns all of the wall recombination to the first molecular vibrational level $v = 0$ and the second one to the last bound vibrational level $v = 32$ of the molecule. In both cases we use $\gamma = 10^{-2}$ (Refs. 9 and 10); the diffusion coefficients are those reported in Refs. 11 and 12.

More realistic values of the partitioning of the recombination energy on the surface over all of the vibrational levels have been recently obtained by Cacciatore et al.[7,8] by using a semiclassical molecular dynamics approach. From this kind of calculation one is able to get the recombination coefficient γ_v on each vibrational level.

The recombination probabilities for O_2 formation in the Eley–Rideal reaction on the silica surface are obtained within the semiclassical collisional method, by solving Hamilton's equations of motion for the oxygen atom, self consistently coupled to the dynamics of the surface atom vibrations.[13,14] The recombination coefficient γ_v is then obtained by averaging the calculated recombination probabilities P_{E-R} over a Maxwell translational energy distribution of the impinging oxygen atom.[7,8] Equation (6) is then rewritten as

$$\left.\frac{\partial C_a}{\partial \eta}\right|_w = \frac{\sum_v \gamma_v}{D}\sqrt{\frac{kT}{2\pi m}} \cdot C_a \tag{8}$$

$$\left.\frac{\partial C_v}{\partial \eta}\right|_w = -\frac{\gamma_v}{D}\sqrt{\frac{kT}{2\pi m}} \cdot C_a \tag{9}$$

Table 1 reports the γ_v coefficients calculated by Cacciatore et al.[7,8]: These values refer to a temperature of 1000 K. In Table 1, the set of the most populated vibrational levels during atom recombination is reported. Note also that the sum is approximately 2×10^{-2}, not far from the experimental global value at 1000 K.

Table 1 Recombination coefficients involving different oxygen vibrational levels

v	γ_v
0	1.05×10^{-3}
5	4.40×10^{-4}
7	8.66×10^{-4}
9	3.95×10^{-4}
10	4.56×10^{-4}
13	1.35×10^{-3}
14	7.78×10^{-4}
15	1.09×10^{-3}
16	3.87×10^{-4}
17	9.04×10^{-4}
18	9.84×10^{-4}
19	1.43×10^{-3}
20	4.82×10^{-4}
21	5.91×10^{-4}
22	1.13×10^{-3}
23	6.53×10^{-4}
24	1.13×10^{-3}
25	9.84×10^{-4}
26	1.12×10^{-3}
27	1.27×10^{-3}
28	9.34×10^{-4}
29	1.17×10^{-3}
30	1.27×10^{-3}
31	8.67×10^{-4}
32	1.09×10^{-3}

Equations and Boundary Conditions

In this section, we discuss the basic equations of our boundary-layer code. The novelty of our code with respect to other boundary layer and Navier–Stokes codes used to simulate reentry problems is the state-to-state approach for vibrational kinetics. Each vibrational level of the ground electronic state of the molecule is considered as a different species described in the boundary layer by its own continuity equation. The vibrational distribution is then calculated step by step along the coordinate normal to the surface. The main result is evidence of nonequilibrium vibrational distributions and their effects on the dissociation–recombination rates as on the temperature gradient normal to the body surface.[1–6,15]

The boundary-layer equations are written in one-dimensional form by using the similarity variables ξ and η as discussed in our previous work[1,2,5,6]:

$$C_v'' + f^* Sc^* C_v' = S_v, \qquad v = 0 \div 33, \qquad \theta'' + f^* Pr^* \theta' = S_T \tag{10}$$

where the unknowns are $C_v = \rho_v / \rho$ and $\theta = T / T_e$ and S_v are the source terms due to the state-to-state vibrational kinetics:

$$O_2(v) + O_2(w) \leftrightarrow O_2(v-1) + O_2(w+1) \tag{11}$$

$$O_2(v) + O_2 \leftrightarrow O_2(v-1) + O_2 \tag{12}$$

$$O_2(v) + O \leftrightarrow O_2(v-1) + O \tag{13}$$

These processes include also the dissociation–recombination gas-phase reactions considered as vibrational–vibrational and vibrational–translational energy exchange processes involving pseudolevel $v = 33$; S_T is the source term for the translational temperature. Note that the use of similarity variables allows us to get information along the normal to the surface at different points near the stagnation point.

Equilibrium boundary conditions at the external edge of the boundary layer have been selected: a fixed temperature T_e given as a parameter and a vibrational distribution satisfying a Boltzmann law at T_e:

$$C_v = (C_v)_{eq} \tag{14}$$

The boundary conditions for the surface have been already discussed. However, when considering a noncatalytic surface, the boundary conditions become a fixed temperature T_w and a zero derivative, with respect to the coordinate η normal to the wall, both for each molecular vibrational level and for the atoms:

$$\left.\frac{\partial C_{v/a}}{\partial \eta}\right|_w = 0 \tag{15}$$

Solution Method

To solve the system of Eqs. (10), the finite difference method is used. As explained in the preceding section, the code is one-dimensional because of the Lees–Dorodnitsyn transformations that change the variables from (x, y) Cartesian variables to (ξ, η) similarity variables. A uniform grid is used to divide the coordinate η

normal to the surface into 80 steps. The derivatives in the system are approximated with central differences. At this stage, the terms obtained from the discretization containing the unknown both in steps $(i-1)$ and $(i+1)$ are inserted in the right-hand side, whereas the terms containing the unknown in step i as well as the source terms are inserted in the left-hand side.

Clearly the nonlinear system is solved in an iterative way: in each step i of a generic iteration the unknowns are calculated taking into account their values both in $(i-1)$, calculated in the previous step of the same iteration, and in $(i+1)$, calculated in the previous iteration. For more details, see Refs. 1, 2, 5, and 6.

Results

To study the importance of an SiO_2 catalytic wall in affecting the kinetic behavior of an oxygen hypersonic flow, different boundary conditions have been considered. In particular four cases will be presented: case 1, noncatalytic wall; case 2, catalytic wall with global recombination in $v=0$; case 3, catalytic wall with global recombination in $v=32$; and case 4, catalytic wall with recombination spread in selected levels. In all cases the external temperature T_e, the wall temperature T_w, the pressure P_e, and $\beta = \mathrm{d}u_e/\mathrm{d}x$ (the derivative of the flow velocity with respect to the coordinate along the surface) have been chosen as fixed parameters ($T_e = 7000$ K, $T_w = 1000$ K, $P_e = 1000$ N/m^2, and $\beta = 5000$ s^{-1}), whose values are typical of reentry conditions, as discussed in our previous work.

In Figs. 1–4 the O_2 vibrational distribution functions obtained considering both a noncatalytic wall (case 1, Fig. 1) and different catalytic walls (cases 2–4, Figs. 2–4) for atom recombination have been reported. The results for a noncatalytic wall (Fig. 1) look similar to those reported for a five species mixture (N_2, N, O_2, O, NO) (Ref. 5). The vibrational distributions present long declining plateaus due to the recombination process in the gas phase. Near the surface (curves 1–2), the plateau is quite stable. Note, however, that the concentration of molecules is very small in all of the points of the boundary layer.

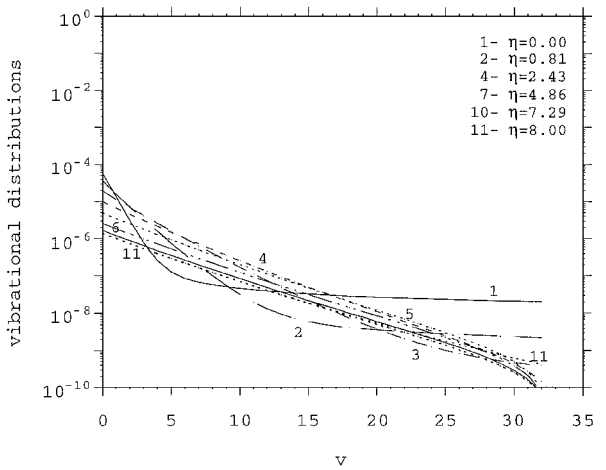

Fig. 1 O_2 vibrational distribution functions along the η coordinate ($\eta = 8$ edge of boundary layer, $\eta = 0$ surface): noncatalytic wall (case 1).

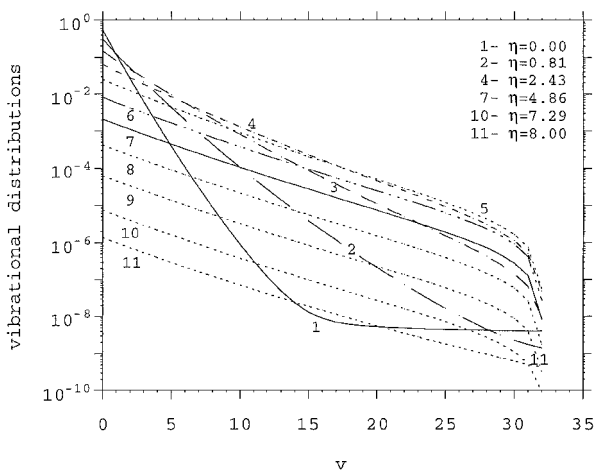

Fig. 2 O_2 vibrational distribution functions: catalytic wall, recombination on $v = 0$ (case 2).

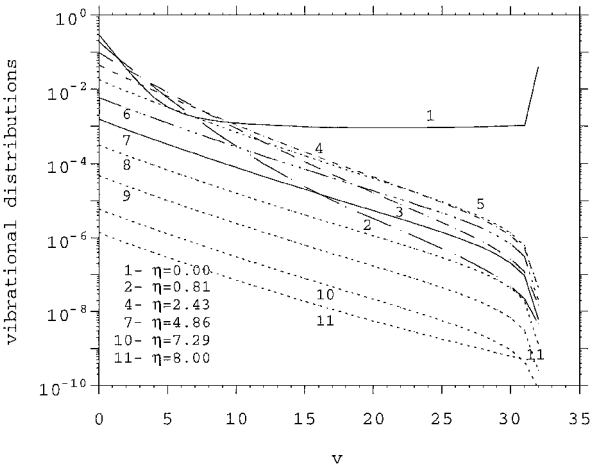

Fig. 3 O_2 vibrational distribution functions: catalytic wall, recombination on $v = 32$ (case 3).

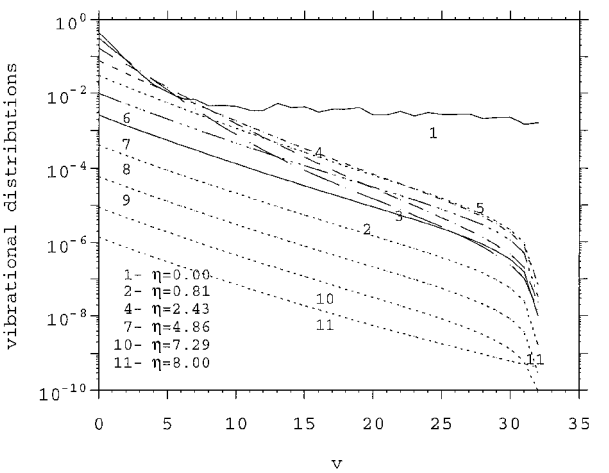

Fig. 4 O_2 vibrational distribution functions: catalytic wall, recombination on each vibrational level (case 4).

The vibrational distributions for the catalytic surface are very similar for cases 2–4 far from the surface. Close to the surface, the results obtained according to model 2 underestimate the vibrational distributions because, in this case, the heterogeneous recombination process does not pump vibrational energy in the desorbing molecules. Models 3 and 4, however, behave similarly. Model 3 pumps vibrational energy on top of vibrational energy (this is the reason why the wall vibrational distribution presents a peak on the last vibrational level); this energy is then redistributed on the whole manifold by gas-phase elementary processes. The results from model 4 present a noncompletely smooth vibrational distribution at the surface due to both the preferential pumping of the heterogeneous process on selected vibrational levels and to the recombination coefficient used, which does not come from an interpolation formula (see Table 1). To stress the differences, in Fig. 5 the vibrational distributions near the surface ($\eta = 0$) calculated according to cases 1–4 are shown.

In Figs. 6 and 7, the O_2 and O concentration profiles along the boundary layer for cases 1–4 are shown. The results indicate a dramatic change, as expected, passing from the noncatalytic to the catalytic surface, that is, from case 1 to cases 2–4. Results obtained from assumptions 2–4 are more similar. Inserting a catalytic surface results in a higher recombination; hence, the O_2 population density (Fig. 6), as well as, of course, the wall vibrational distribution function (Fig. 5), increases; on the other side, the O population density at the wall decreases.

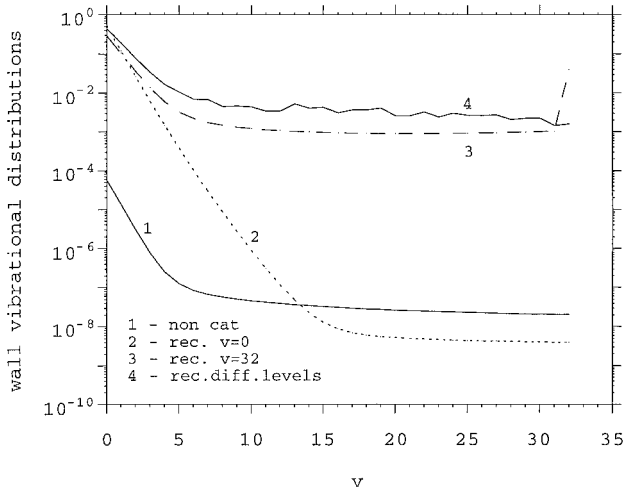

Fig. 5 O_2 vibrational distribution functions at the wall for the different cases.

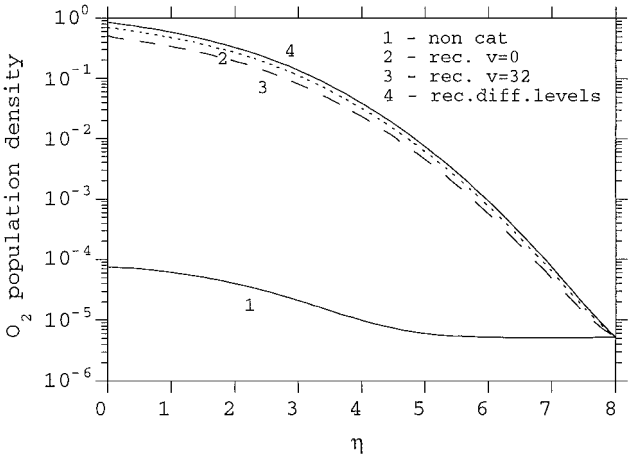

Fig. 6 O_2 total population density vs η for the different cases.

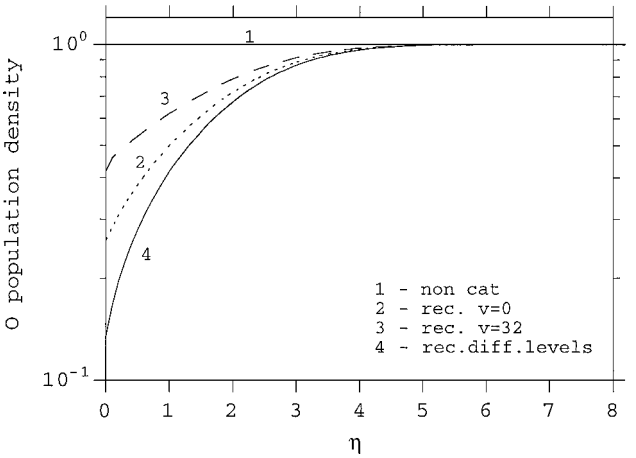

Fig. 7 O total population density vs η for the different cases.

Results obtained in cases 3 and 4 demonstrate that catalysis simulating a recombination on different vibrational levels (case 4) is more effective: This means less atoms and more molecules, as well as higher vibrational distribution functions at the surface. To estimate the importance of the differences obtained in cases 3 and 4, it is useful to study the corresponding heat fluxes. Thus, in Fig. 8, the temperature gradient along the coordinate η normal to the surface, for cases 1–4, has been plotted. The gradient suddenly increases near the catalytic surface either with global recombination on the last vibrational level (case 3) or with recombination on selected

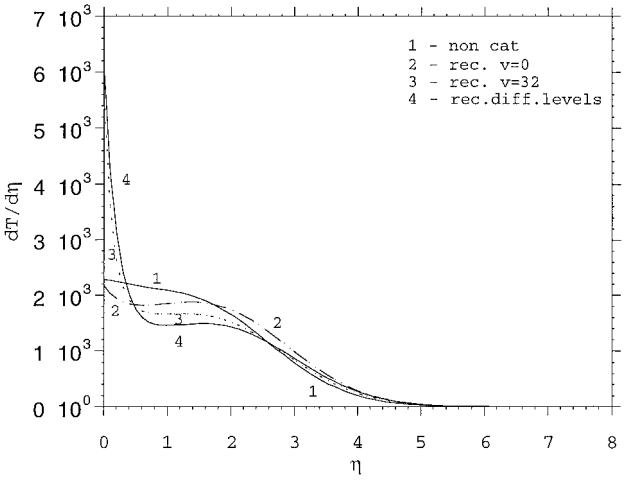

Fig. 8 Temperature gradient vs η for the different cases.

vibrational levels (case 4), and the differences between these two cases are not very important.

Remembering that the Fourier part of the heat flux is proportional to the temperature gradient

$$q_F = -\lambda' \frac{\partial T}{\partial \eta} \tag{16}$$

(with λ' the thermal conductivity coefficient) and that in the conditions under investigation the difference between the total heat flux and the Fourier part does not exceed 8% (see Ref. 15), we may conclude that for heat flux studies the phenomenological model with recombination on the last vibrational level (case 3) is a good approximation to catalytic surfaces.

Role of a Deactivating Surface

To further improve the code and to better simulate a real silica surface, not only catalysis but also deactivation and dissociation on the surface should be inserted. Therefore, the wall boundary conditions [Eqs. (8) and (9)] transform as

$$\left.\frac{\partial C_a}{\partial \eta}\right|_w = \frac{\sum_v \gamma_v}{D}\sqrt{\frac{kT}{2\pi m}} \cdot C_a - \sum_v \gamma_{\text{diss}} C_v \tag{17}$$

$$\left.\frac{\partial C_v}{\partial \eta}\right|_w = -\frac{\gamma_v}{D}\sqrt{\frac{kT}{2\pi m}} \cdot C_a + \gamma_{\text{diss}} \cdot C_v - \gamma_{\text{deact}} \cdot C_v + \gamma_{\text{deact}} \cdot C_{v+1} \tag{18}$$

Note that in the right-hand side of Eqs. (17) and (18), the first term is due to catalysis, the second one to dissociation, and the third and fourth ones [only in Eq. (18)] to deactivation. For the last process we consider only one quantum deactivation, that is,

$$O_2(v) + \text{wall} \rightarrow O_2(v-1) + \text{wall} \tag{19}$$

It is straightforward that the third term in the right-hand side of Eq. (18) is due to the loss of the molecule $O_2(v)$ in the Eq. (19) process, whereas the fourth term is due to the gain of the molecule $O_2(v)$ in the corresponding process, $O_2(v+1) + \text{wall} \rightarrow O_2(v) + \text{wall}$.

An estimation of dissociation and deactivation probabilities has been performed by using the semiclassical trajectory method. These calculations, which have been restricted to $v = 21$, show that the vibrational relaxation of $O_2(v)$ hitting the silica surface is strongly quenched. The dissociation probability for the inelastic and dissociative process for $O_2(v = 21)$ is close to unity ($\gamma_{\text{diss}} = 0.8$) at $E_{\text{kin}} = 0.007$ eV as well as at $E_{\text{kin}} = 0.07$ eV when the surface temperature is 1000 K. From the same calculations, a reasonable value of 10^{-3} for γ_{deact} has been estimated for the process in Eq. (19). The

large dissociation constants of the vibrationally excited levels are in line with the experimental observation of the enhanced reactivity of vibrationally excited NO impinging a Cu surface.[16]

Dissociation and deactivation probabilities for all $O_2(v)$ levels have been considered equal to those involving level $v = 21$. This procedure probably overestimates the dissociation probability and at the same time underestimates the deactivating probability. These probabilities have been inserted in the boundary equations (17) and (18), and the resulting vibrational distributions are shown in Fig. 9. To better understand the role of both dissociation and deactivation, the wall vibrational distributions obtained inserting a simply catalytic (curve 1), a catalytic and deactivating (curve 2), a catalytic and dissociating (curve 3), and finally a catalytic, deactivating, and dissociating (curve 4) surface are shown in Fig. 10. O_2 and O population densities vs η, in the same cases as in Fig. 10, are plotted in Figs. 11 and 12, respectively. As expected, the selected probabilities maximize the role of dissociation on the vibrational distributions and at the same time minimize the role of vibrational deactivation. Future work in this direction should provide a complete set of dissociation and deactivation probabilities, the last including multiquantum jumps.

In any case, nonequilibrium vibrational distributions appear near the surface. These distributions could create electrons through associative ionization from high lying vibrational levels. In turn electrons can promote the boundary-layer chemistry through many electron impact collisions. These effects are, however, beyond the scope of the present paper and are left to future work.

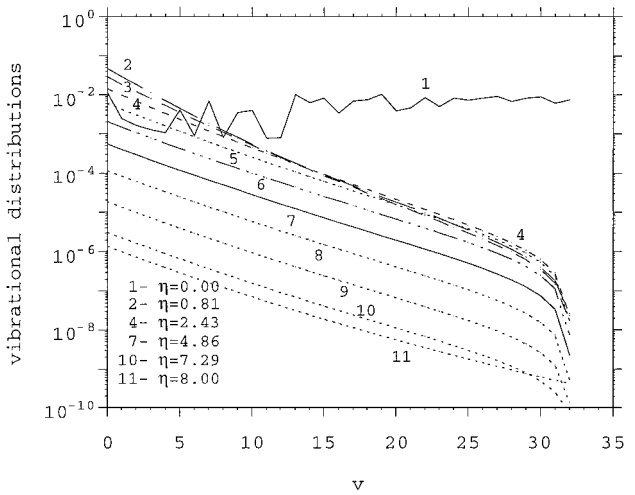

Fig. 9 O_2 vibrational distribution functions: catalytic, dissociating, and deactivating wall.

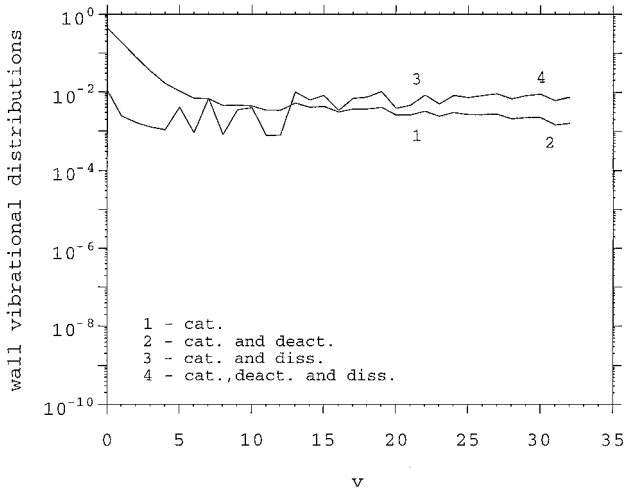

Fig. 10 O_2 vibrational distribution functions at the wall for different cases.

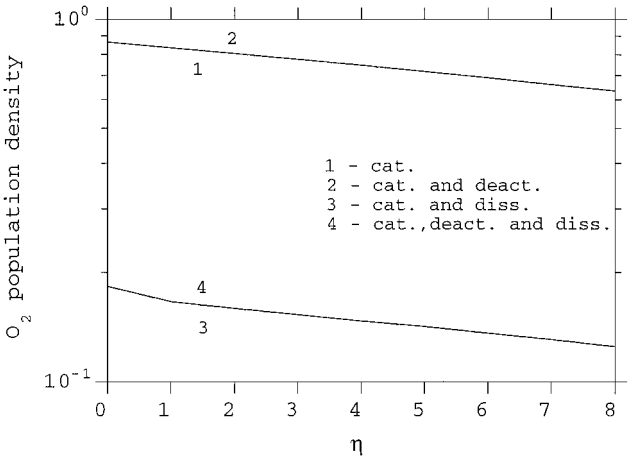

Fig. 11 O_2 total population density vs η for different cases.

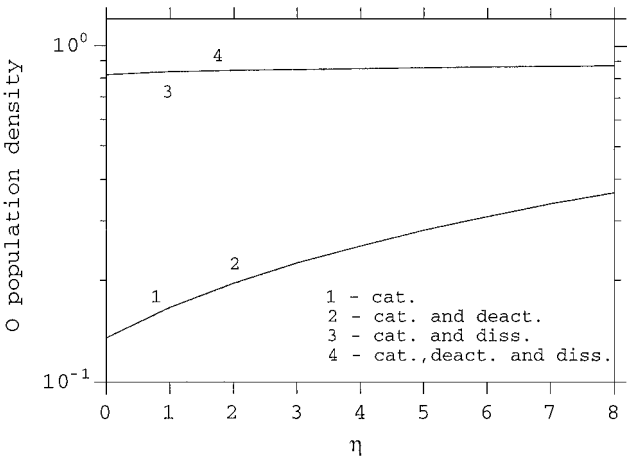

Fig. 12 O total population density vs η for different cases.

Conclusions

The results of this study emphasize the role of a catalytic surface in affecting the vibrational distributions of O_2 near the surface. The different catalytic models used show a substantial agreement between case 3 (phenomenological) and case 4 (theoretical). This result is quite important because apparently one can use experimental catalytic recombination rates to pump the top of the vibrational ladder. This conclusion is in line with what happens in the gas phase.

As a final comment, we want to stress the importance of state-to-state kinetics compared with the global kinetics involving only the last vibrational level of the molecule. Indeed, the two treatments are equivalent from the point of view of heat transfer; however, other macroscopic quantities such as total atomic oxygen and molecular oxygen concentrations are affected by the selected model. Regarding the dissociation and the deactivation on the surface, it seems that only the dissociation affects the O_2/O kinetics.

It is reasonable to predict that, when considering air, due to the N_2 reactivity, the catalytic surface could affect both the heat flux and the kinetics, leading to a non-Boltzmann behavior of the vibrational distributions as well as to a non-Arrhenius behavior of the rate constants.

Acknowledgment

This work has been partially supported by Agenzia Spaziale Italiana.

References

[1] Armenise, I., Capitelli, M., Celiberto, R., Colonna, G., and Gorse, C., "Non-equilibrium Vibrational Distributions of N_2 Under Reentry Conditions: The Role of Atomic Nitrogen," AIAA Paper 94-1987, June 1994.

[2] Armenise, I., Capitelli, M., and Gorse, C., "On the Coupling of Non-equilibrium Vibrational Kinetics and Dissociation–Recombination Processes in the Boundary Layer Surrounding an Hypersonic Reentry Vehicle,"

Proceedings of the ESA (European Space Agency) Second European Symposium on Aerothermodynamics for Space Vehicles, SP-367, ESA, Noordwijk, The Netherlands, 1995, pp. 287–292.

[3]Capitelli, M. (ed.), *Molecular Physics and Hypersonic Flows*, Kluwer Academic, Dordrecht, The Netherlands, 1996, pp. 703–716.

[4]Armenise, I., Capitelli, M., Colonna, G., and Gorse, C., "Nonequilibrium Vibrational Kinetics in the Boundary Layer of Reentering Bodies," *Journal of Thermophysics and Heat Transfer*, Vol. 10, No. 3, 1996, pp. 397–405.

[5]Capitelli, M., Armenise, I., and Gorse, C., "State to State Approach in the Kinetics of Air Components Under Reentry Conditions," *Journal of Thermophysics and Heat Transfer*, Vol. 11, No. 4, 1997, pp. 570–578.

[6]Armenise, I., Capitelli, M., and Gorse, C., "Nitrogen Nonequilibrium Vibrational Distributions and Non-Arrhenius Dissociation Constants in Hypersonic Boundary Layers," *Journal of Thermophysics and Heat Transfer*, Vol. 12, No. 1, 1998, pp. 45–51.

[7]Cacciatore, M., Rutigliano, M., and Billing, G. D., "Energy Exchanges, Recombination Coefficients and Dynamics for Oxygen Recombination on Silica Surfaces," AIAA Paper 98-2843, June 1998.

[8]Cacciatore, M., Rutigliano, M., and Billing, G. D., "Eley–Rideal and Langmuir–Hinshelwood Recombination Coefficients for Oxygen on Silica Surfaces," *Journal of Thermophysics and Heat Transfer*, Vol. 13, No. 2, 1999, pp. 195–203.

[9]Nasuti, F., Barbato, M., and Bruno, C., "Material-Dependent Catalytic Recombination Modeling for Hypersonic Flows," *Journal of Thermophysics and Heat Transfer*, Vol. 10, No. 1, 1996, pp. 131–136.

[10]Barbato, M., and Bruno, C., "Heterogeneous Catalysis: Theory, Models and Applications," *Molecular Physics and Hypersonic Flows*, edited by M. Capitelli, Kluwer Academic, Norwell, MA, 1996, pp. 139–160.

[11]Levin, E., Partridge, H., and Stallcop, J. R., "High Temperature Transport Properties of Air," AIAA Paper 87-1632, June 1987.

[12]Capitelli, M., Gorse, C., Longo, S. and Giordano, D., "Collision Integrals of High-Temperature Air Species," *Journal of Thermophysics and Heat Transfer*, Vol. 14, No. 2, 2000, pp. 259–268; also AIAA Paper 98-2936, June 1998.

[13]Billing, G. D., "The Dynamics of Molecule–Surface Interactions," *Computational Physics Report*, Vol. 12, No. 6, 1990, pp. 383–450.

[14]Cacciatore, M., and Billing, G. D., "Dynamical Relaxation of H2(v,j) on a Copper Surface," *Surface Science*, Vol. 232, No. 1–2, 1990, pp. 35–50.

[15]Armenise, I., Cacciatore, M., Capitelli, M., Rutigliano, M., Kustova, E., and Nagnibeda, E., "The Influence of Non-Equilibrium Vibrational and Dissociation–Recombination Kinetics on the Heat Transfer and Diffusion in the Boundary Layer Under Reentry Conditions," *Rarefied Gas Dynamics*, Vol. 2, edited by R. Brun, R. Champagne, R. Gatignol, and J. C. Lengrand, Cepadues, Toulouse, France, 1999, pp. 273–280.

[16]Hou, H., Huang, Y., Gulding, S. J., Rettner, C. T., Auerbach, D. J., and Wodtke, A. M., "Enhanced Reactivity of Highly Vibrationally Excited Molecules on Metal Surfaces," *Science*, Vol. 284, June 1999, pp. 1647–1650.

I. D. Boyd
Associate Editor